spectrometer with a single dispersing crystal with $\mu \simeq 0$ (*i.e.* a 'perfect' crystal) and a source of very small dimension in the plane of diffraction then a 'film' profile with $s = 0$ has twice the angular dispersion of the 'counter' profile (see Fig. 1*b*). This suggests the possibility of increasing the numerical dispersion of the 'film' profile by using a non-standard 'inverse' scan mode with $s = -1, -2$, *etc.* to increase the effective dispersion relative to the 'counter' profile by 3, 4, *etc.*

We are most grateful to Dr S. L. Mair for allowing us to use her K_2SnCl_6 specimen. One of us (AWS) acknowledges the financial support of a CSIRO Postdoctoral Award.

References

ALEXANDER, L. E. & SMITH, G. S. (1962). *Acta Cryst.* **15**, 983-1004.
ARNDT, U. W. & WONACOTT, A. J. (1977). *The Rotation Method in Crystallography.* Amsterdam: North-Holland.
DENNE, W. A. (1977). *Acta Cryst.* A**33**, 987-992.
EHRENBERG, W. & MARK, H. (1927). *Z. Phys.* **42**, 807-822.
HOYT, A. (1932). *Phys. Rev.* **40**, 477-483.
JAMES, R. W. (1948). *The Optical Principles of the Diffraction of X-rays.* London: Bell.
MATHIESON, A. McL. (1982). *Acta Cryst.* A**38**, 378-382.
MATHIESON, A. McL. (1983*a*). *J. Appl. Cryst.* **16**, 257-258.
MATHIESON, A. McL. (1983*b*). *Acta Cryst.* A**39**, 79-83.
MATHIESON, A. McL. (1984*a*). *Acta Cryst.* A**40**, 355-363.
MATHIESON, A. McL. (1984*b*). *Aust. J. Phys.* **37**, 55-61.
MATHIESON, A. McL. (1985). *Acta Cryst.* A**41**, 309-316.
MATHIESON, A. McL. & STEVENSON, A. W. (1984). *Aust. J. Phys.* **37**, 657-665.
MATHIESON, A. McL. & STEVENSON, A. W. (1985). *Acta Cryst.* A**41**, 290-296.
MATHIESON, A. McL. & STEVENSON, A. W. (1986). *Acta Cryst.* A**42**, 223-230.
PARRATT, L. G. (1936). *Phys. Rev.* **50**, 1-15.
SCHNEIDER, J. R. (1977). *Acta Cryst.* A**33**, 235-243.
SCHOENBORN, B. P. (1983). *Acta Cryst.* A**39**, 315-321.
WOOSTER, N. (1945). *J. Sci. Instrum.* **22**, 132.

Acta Cryst. (1986). A**42**, 441-449

On the Theory of Six-Beam X-ray Spherical-Wave Diffraction

BY V. G. KOHN

I. V. Kurchatov Institute of Atomic Energy, 123182, *Moscow, USSR*

AND A. H. TONEYAN

Department of Physics, Erevan State University, Erevan, USSR

(*Received* 20 *October* 1983; *accepted* 27 *March* 1986)

Abstract

A general formula is obtained for the intensity distribution in the film behind a single crystal in the case of spherical-wave X-ray multiple diffraction. The theory takes into account the phase shift of the waves not only inside the crystal but also in the vacuum before and after the crystal along the wave path source-crystal-film of length L. The topographic images are calculated in the case of (220/242/044/$\bar{2}$44/$\bar{2}$02) six-beam diffraction of Cu $K\alpha$ radiation in a germanium crystal of thickness 0·2 mm for different values of L. The enhancement of the anomalous transmission effect is weakly displayed on the topographs because of strong scattering of the radiation inside the crystal. The intensity distribution depends on L. The possibility is shown of focusing X-rays to a considerable extent.

1. Introduction

In recent years the scheme shown in Fig. 1 has been widely used for experimental investigations of X-ray multiple diffraction in single crystals. The divergent radiation of the microbeam X-ray tube falls directly on a crystal in the form of a plate with thickness t. The intensity of diffracted beams is determined by the darkening of the film placed behind the crystal [see, for example, the papers by Balter, Fildman & Post (1971), Huang & Post (1973), Kshevetskii & Mihailyuk (1976), Mihailyuk, Kozmik & Kshevetskii (1977)]. To enlarge the section of the topographs corresponding to multiple-beam angles of incidence

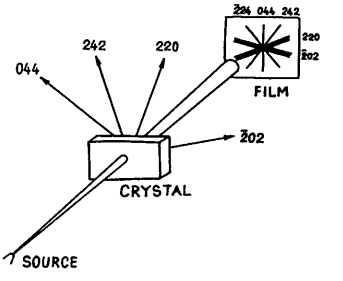

Fig. 1. Scheme of the experiment for investigating X-ray multiple diffraction.

0108-7673/86/060441-09$01.50

of radiation on the crystal, the distance L between the source and the film has been made as large as possible (up to two metres). The above authors all compared the topographs with patterns of angular dependence of intensity calculated with the conventional theory of plane-wave X-ray multiple diffraction. Though such an approach provides a certain qualitative (mainly geometrical) correspondence between theory and experiment, more detailed analysis detects a difference between them.

The principal inconsistency of this approach was pointed out by Afanas'ev & Kohn (1977*a*). They carried out a more correct calculation of topographic images for the experimental arrangement described above. The spherical-wave X-ray diffraction theory was developed and the two-beam case considered as an example. This theory takes into account the phase shift of the waves not only inside the crystal but also in the vacuum before and after the crystal. It was shown that the diffraction pattern depends considerably on the ratio L/t. Further experimental investigations (Aristov, Polovinkina, Shmyt'ko & Shulakov, 1978; Kozmik & Mihailyuk, 1978; Aristov, Polovinkina, Afanas'ev & Kohn 1980) verified completely all the effects predicted by the theory, in particular, the phenomenon of the focusing of the weakly absorbed field at a certain value of L/t.

The general theory of spherical-wave X-ray multiple diffraction has been developed by Kohn (1977). The theory takes into account the distance L and the nonmonochromaticity of the radiation. However, the formula for the distribution of intensity in the film turned out to be a very difficult one for carrying out direct numerical calculations.

The purpose of the present paper is to develop further the theory formulated by Kohn (1977). Here a simpler approximation is worked out which makes it possible to calculate the topographic images by the same methods as in the plane-wave case, but taking into account the curvature of the incident spherical-wave front. The latter factor, as well as the curvature of the dispersion surface, are included in computations in the approximation of a stationary-phase method (Jeffreys & Swirles, 1966) extended for two-fold integrals. At those points of the topograph where the stationary-phase method is incorrect (the points of focusing), the computation was carried out more accurately.

The derivation of the formulae for describing the intensity distribution of the forward direct beam is given in § 2. Computational aspects are discussed in § 3. We carried out the computation of topographic images for the case of (220/242/044/$\bar{2}$24/$\bar{2}$02) six-beam diffraction of Cu $K\alpha$ radiation in a Ge plate with $t = 0{\cdot}2$ mm for different values of L (§ 4). We note that the results presented constitute the first attempt to analyse the case of spherical-wave X-ray multiple diffraction on the basis of a physically realistic theory which takes into account the distance between the source and the film. A rather difficult case is considered as an example, because the greatest divergence occurs between the experimental results and theoretical predictions which do not take into account the phase shift of the waves (Huang, Tillinger & Post, 1973).

2. General formulation

2.1. *Initial formulae*

Let the X-ray spherical wave with frequency ω fall on a crystal plate of thickness t. The crystal is orientated so that the wave vector $\boldsymbol{\kappa}_0$, the magnitude of which is equal to $K = \omega/c = 2\pi/\lambda$, satisfies the conditions of multiple diffraction. It is convenient to use the following integral form of the spherical wave in a half-space $\mathbf{r}\boldsymbol{\kappa}_0 > 0$ (Kato, 1961):

$$\exp(iKr)/ir = \int (\mathrm{d}\mathbf{q}/2\pi) \exp[i\mathbf{q}\mathbf{r} + i\boldsymbol{\kappa}_0\mathbf{r}(1-q^2/K^2)^{1/2}] \times (K^2-q^2)^{-1/2} \quad (1)$$

where integration is to be carried out over all values of the vector $\mathbf{q}$ in a plane perpendicular to $\boldsymbol{\kappa}_0$. Since the multiple diffraction takes place in a narrow cone near $\boldsymbol{\kappa}_0$ (see Fig. 1), only vectors $\mathbf{q}$ of small magnitude $q \ll K$ are of interest. That is why K can be substituted for $(K^2-q^2)^{1/2}$ in the denominator of the integrand, and the numerator may be given in the form of $\exp[i\mathbf{K}_0(\mathbf{q})\mathbf{r}]$, where

$$\mathbf{K}_0(\mathbf{q}) \simeq \boldsymbol{\kappa}_0(1-q^2/2K^2) + \mathbf{q}. \quad (2)$$

Then it is necessary to solve the multiple diffraction problem for an incident plane wave with the wave vector $\mathbf{K}_0$. The solution is given by Pinsker (1978, p. 442). Details may be found in this reference; we give a final expression for the induction vector of the spherical-wave electromagnetic field beyond the crystal in the forward-transmitted beam (Kohn, 1977) (we use Pinsker's notation, but with difference in signs).

$$\mathbf{D}_0^{(d)}(\mathbf{r}) = \gamma_0^{1/2} \sum_{ss'} D_{0s}^{(a)} F_{00}^{ss'}(\mathbf{r}) \mathbf{e}_{0s'}. \quad (3)$$

Here $\mathbf{e}_{0s}$ are polarization vectors ($s = \pi, \sigma$), $D_{0\pi}^{(a)}$, $D_{0\sigma}^{(a)}$ are the magnitudes of incident-wave induction-vector components which are parallel to $\mathbf{e}_{0\pi}$, $\mathbf{e}_{0\sigma}$ respectively, $\gamma_0 = \boldsymbol{\kappa}_0\mathbf{n}/K$, $\mathbf{n}$ is an inner normal to a crystal surface,

$$F_{00}^{ss'}(\mathbf{r}) = \int (\mathrm{d}\mathbf{q}/2\pi K) \exp[i\mathbf{K}_0\mathbf{r}] \times \sum_j B_{0s}^{(j)} B_{0s'}^{(j)} \exp[-iK\delta^{(j)}t], \quad (4)$$

$B_{0s}^{(j)}(\mathbf{q})$ and $\delta^{(j)}(\mathbf{q})$ are the eigenvector and eigenvalue number j of the matrix for multiple diffraction of X-rays by a crystal (Pinsker, 1978):

$$\sum_{ms'} G_{nm}^{ss'} B_{ms'} = \delta B_{ns}. \quad (5)$$

Indexes n and m have values from 0 to 5 in a six-beam case and label the direct and diffracted beams respectively.

Let $\mathbf{x}=(x_1, x_2)$ be a two-dimensional vector that defines some point on the film plane. This plane is perpendicular to an incident beam. The distance between a point source and the film is L. Then the intensity of nonpolarized radiation at a point $\mathbf{x}$, normalized to the intensity in vacuum for $L=1$ m, is defined by the expression

$$I_0^{(d)}(\mathbf{x}, L, t)=\tfrac{1}{2}\sum_{ss'}|\sum_j F_j^{ss'}(\mathbf{x}, L, t)|^2, \quad (6)$$

where

$$F_j^{ss'}(\mathbf{x}, L, t)=\int(\mathrm{d}\mathbf{q}/2\pi K) f_j^{ss'}(\mathbf{q}, t) \times \exp[i\varphi_j(\mathbf{q}, \mathbf{x}, t, L)], \quad (7)$$

$$f_j^{ss'}(\mathbf{q}, t)=B_{0s}^{(j)}(\mathbf{q})B_{0s'}^{(j)}(\mathbf{q})\exp[-\mu_j(\mathbf{q})t/2]. \quad (8)$$

Here $\mu_j(\mathbf{q})=-2K\,\mathrm{Im}[\delta^{(j)}(\mathbf{q})]$ is the absorption coefficient of the jth zone of the X-ray multiwave field (*i.e.* of the jth X-ray standing wave). Despite the fact that the matrix G is complex, it is sufficient to solve only for the real part of (5) corresponding to the case of a nonabsorbing crystal (Pinsker, 1978; Kohn, 1976). The absorption coefficient μ_j is determined by

$$\mu_j=\sum_{\substack{nm\\ss'}} B_{ns}^{(j)}(G_i)_{nm}^{ss'}B_{ms'}^{(j)}, \quad (9)$$

where G_i is the imaginary part of G. We shall use below the notation $\delta^{(j)}$ only for the real part of this quantity, which can be obtained from (5) in the case of a nonabsorbing crystal. The important role in understanding the diffraction pattern is played by the phase, determined by

$$\varphi_j(\mathbf{q}, \mathbf{x}, t, L)=\mathbf{qx}-q^2L/2K-K\delta^{(j)}(\mathbf{q})t. \quad (10)$$

2.2. *Stationary-phase method*

The most interesting situation arises when all three terms on the right-hand side of (10) are of the same order of magnitude. The multiple diffraction of X-rays takes place in the angular region $|\theta|<0{\cdot}06$ mrad, where $\boldsymbol{\theta}=\mathbf{q}/K$. Taking into consideration that the change of phase in this region due to the second term is of order 10^2 at typical values of parameters $L=1$ m and $\lambda=0{\cdot}1$ nm, we can use the stationary-phase method (Jeffreys & Swirles, 1966) for finding the approximate value of the integral (7).

The idea of the method is as follows. Let us assume that the function $f_j^{ss'}(\mathbf{q})$ changes slowly compared with $\exp[i\varphi_j(\mathbf{q})]$. Then the main contribution to the integral is given by the integration region where the phase change is smallest. Let the point $\mathbf{q}_0=(q_1^{(0)}, q_2^{(0)})$ satisfy the conditions

$$\partial\varphi_j/\partial q_k=x_k-q_kL/K-Kt[\partial\delta^{(j)}(\mathbf{q})/\partial q_k]=0 \quad (11)$$

where $k=1, 2$. The region near the point $\mathbf{q}_0$ is of just that kind. In this region the expansion for the phase φ_j through terms of the order of the components of a two-dimensional vector $\mathbf{u}=(\mathbf{q}-\mathbf{q}_0)$ has the form

$$\varphi_j(\mathbf{u})=\varphi_j(\mathbf{q}_0)+\tfrac{1}{2}\sum_{k,l=1}^{2}\alpha_{kl}^{(j)}u_ku_l + \tfrac{1}{6}\sum_{k,l,m=1}^{2}\beta_{klm}^{(j)}u_ku_lu_m+\cdots \quad (12)$$

where

$$\alpha_{kl}^{(j)}=(\partial^2\varphi_j/\partial q_k\,\partial q_l)_{\mathbf{q}=\mathbf{q}_0} =-\delta_{kl}L/K-Kt[\partial^2\delta^{(j)}(q)/\partial q_k\,\partial q_l]_{\mathbf{q}=\mathbf{q}_0}, \quad (13)$$

$$\beta_{klm}^{(j)}=(\partial\alpha_{kl}^{(j)}/\partial q_m)_{\mathbf{q}=\mathbf{q}_0}.$$

Substituting a constant $f_j(\mathbf{q}_0)$ for the function $f_j(\mathbf{q})$ and using only the first two terms of (12), we have the following approximation for the contribution of this region

$$\Delta F_j^{ss'}(\mathbf{x})\simeq\{f_j(\mathbf{q}_0)\exp[i\varphi_j(\mathbf{x}, \mathbf{q}_0)]/2\pi K\} \times\int\mathrm{d}\mathbf{u}\exp\left[(i/2)\sum_{k,l}\alpha_{kl}^{(j)}u_ku_l\right]. \quad (14)$$

The integral in (14) should strictly be calculated over some region of values u_1 and u_2 near the zero point. However, since the large values of u_k give a small contribution to the integral due to the rapid oscillations in the integrand, we may extend the integration over the entire range of coordinates. In this case the integral is calculated analytically.

Let us turn the axes of the coordinate system on the plane of a two-dimensional vector $\mathbf{u}$ by some angle ψ so that for the new variable $\tilde{u}_k$ the matrix $\tilde{\alpha}_{kl}^{(j)}$ becomes a diagonal one, $\tilde{\alpha}_{kl}^{(j)}=\delta_{kl}A_k^{(j)}$, where δ_{kl} is Kronecker's symbol. The transition from old variables to the new ones is made with the matrix

$$\sigma_{km}=\begin{pmatrix}\cos\psi & -\sin\psi\\ \sin\psi & \cos\psi\end{pmatrix}, \quad \tan 2\psi=2\alpha_{12}/(\alpha_{11}-\alpha_{22}). \quad (15)$$

The diagonal elements of the matrix $\tilde{\alpha}=\sigma^{-1}\alpha\sigma$ are then given by

$$A_{1,2}^{(j)}=\tfrac{1}{2}\{\alpha_{11}+\alpha_{22}\pm\mathrm{sign}\,(\alpha_{11}-\alpha_{22}) \times[(\alpha_{11}-\alpha_{22})^2+4\alpha_{12}^2]^{1/2}\}. \quad (16)$$

As a result, the integral in (14) is

$$J_1J_2=\int\mathrm{d}\tilde{u}_1\exp[i(A_1/2)\tilde{u}_1^2]\int\mathrm{d}\tilde{u}_2\exp[i(A_2/2)\tilde{u}_2^2] =(2\pi i/A_1)^{1/2}(2\pi i/A_2)^{1/2}. \quad (17)$$

The approximation described is used in the stationary-phase method for estimating integrals when there are rapid oscillations in the integrand. This approximation gives an overestimate for the result at those

values of the parameters where either A_1 or A_2 becomes anomalously small. At the points where $A_1 = 0$ or $A_2 = 0$, we obtain a divergent result. In our case, one knows that this divergence is connected with the effect of focusing the X-rays within some range of angles of incidence $\boldsymbol{\theta} = \mathbf{q}/K$. Actually, coordinates of the point on the topograph corresponding to the vector $\mathbf{q}$ in accordance with (11) are

$$x_k = q_k L/K + Kt[\partial\delta^{(j)}(\mathbf{q})/\partial q_k]. \quad (18)$$

It can be shown after the transition to a new coordinate system that the x coordinates do not change with change of coordinate $\tilde{u}_k$ in the plane of the vectors $\mathbf{q}$ if the condition $A_k = 0$ is fulfilled.

In order to estimate the integral in (7) for this case, it is necessary to take into account the next term in the expansion of the phase in powers of $\tilde{u}_1$ (12). If, for example, the parameter A_1 is anomalously small and another parameter has a value close to the average, then the corresponding integral is approximately

$$\int d\tilde{u}_1 \exp[i(A_1/2)\tilde{u}_1^2 + i(H_1/6)\tilde{u}_1^3] = J_1(A_1, H_1) \quad (19)$$

where

$$H_1 = \tilde{\beta}_{111} = \beta_{111}C^3 + \beta_{222}S^3 + 3\beta_{112}C^2S + 3\beta_{122}CS^2. \quad (20)$$

The notation $C = \cos\psi$, $S = \sin\psi$ is used in (20). The limits of integration in (19) cannot be extended to infinity at all values of A_1, because the main contribution is given not only by the region with its centre at the point $\tilde{u}_1 = 0$, but also by the region with the point $\tilde{u}_1 = 2A_1/H_1$ as centre. That is why to estimate the magnitude of the integral we have used the following interpolation approximation:

$$|J_1(A_1, H_1)| = [|J_1(A_1, 0)|^{-1} + |J_1(0, H_1)|^{-1}]^{-1}, \quad (21)$$

where

$$|J_1(A_1, 0)|^{-1} = |A_1/2\pi|^{1/2} = 0{\cdot}3989|A_1|^{1/2}, \quad (22)$$

$$|J_1(0, H_1)|^{-1} = |H_1/6|^{1/3}3^{1/2}/\Gamma(\tfrac{1}{3}) = 0{\cdot}3558\,|H_1|^{1/3}. \quad (23)$$

In (23) $\Gamma(x)$ is the gamma function.

These considerations are obviously true where A_2 is anomalously small and A_1 is large enough. Here we get the same formulae (19)–(23) for J_2 (A_2, H_2) after permutation of the indexes 1 and 2 and the substitution of $-\psi$ for ψ. The case where $A_1 = 0$ and $A_2 = 0$ in one and the same topograph point requires special treatment, because the integral does not equal $J_1(0, H_1)J_2(0, H_2)$. Nevertheless, this product is finite and the error caused by its use instead of a more correct value is small. It should be noted that such situations arise extremely infrequently.

In general, several angular regions can contribute to one point on the topograph, depending on the structure of the dispersion surface (DS) and the distance L. In this case we must add the contributions from all these regions. The intensity then involves the terms which correspond to an interference of different zones of the DS (the terms with $j \neq j'$ in the sum over j and j') and of different angular regions within any zone. We note that the interference terms in the intensity oscillate strongly with a change of x coordinate in the small region. Only a mean pattern without interference terms is fixed in the experiment shown in Fig. 1.

If the above approximations are taken into account, it is easy to transform the initial expression (6) to the following:

$$I_0^{(d)}(\mathbf{x}, t, L) \simeq \sum_{ij}[I_{0j}^{pw}(\mathbf{q}_{ij}, t)/D_{1j}^2(\mathbf{q}_{ij})D_{2j}^2(\mathbf{q}_{ij})], \quad (24)$$

where

$$I_{0j}^{pw}(\mathbf{q}, t) = \tfrac{1}{2}\left\{\sum_s [B_{0s}^{(j)}(\mathbf{q})]^2\right\}^2 \exp[-\mu_j(\mathbf{q})t] \quad (25)$$

$$D_{mj}(\mathbf{q}, t, L) = |L - C_m^{(j)}(\mathbf{q})t|^{1/2} + 0{\cdot}89187K^{1/2}|H_m^{(j)}(\mathbf{q}, t)|^{1/3} \quad (26)$$

$$C_m^{(j)}(\mathbf{q}) = [KA_m^{(j)}(\mathbf{q}) + L]t^{-1}, \qquad m = 1, 2. \quad (27)$$

Here the coefficient $C_m^{(j)}(\mathbf{q})$ does not depend on t and L. According to (24), the intensity of radiation at the point $\mathbf{x}$ on the topograph is determined by all the points in the $\mathbf{q}$ plane which satisfy (11) for each zone of the DS. The index j, as before, refers to zones of the DS, and index i numbers the different solutions of (11) for each zone. Since we consider only the real roots of (11), the number of terms in the sum over i is in general different for the different zones of DS. Despite its apparent simplicity, (24) describes a complicated intensity distribution on the topograph due to the dependence of $\mathbf{q}_{ij}$ on x, t and L, which reflects the intricate form of the DS.

2.3. *Limiting cases*

We consider now the limiting cases. Let L/t be very large. Then $D_m \simeq L^{1/2}$ and the $\mathbf{q}_{ij}$, according to (11), are equal approximately to $K\mathbf{x}/L$. Therefore, the intensity distribution on the topographs is described by a simpler expression,

$$I_0^{(d)}(\mathbf{x}) \simeq (1/L^2)\sum_j I_{0j}^{pw}(K\mathbf{x}/L, t). \quad (28)$$

According to (28), the topographs show the angular dependence of the intensity in the incident-plane-wave case on $\mathbf{x}/L$ rather than on an angular variable. In the real experiment, where $L \lesssim 2$ m, the case mentioned does not occur (see below).

If $L = 0$, we obtain the opposite limiting case (the source is placed on the entrance surface and the film is placed on the exit surface of a crystal). We note that the well known theory by Kato (1961, 1968) of

two-beam X-ray spherical-wave diffraction corresponds to just this case. From (18), the dimensions of the diffraction pattern are now proportional to t and its form is determined by the form of the DS. In the two-beam case, as is well known (Kato, 1968), all the radiation is concentrated inside a triangle (the Borrmann fan). In the six-beam case the radiation is concentrated inside a pyramid with its base in the form of a hexagon of reciprocal-lattice vectors and with its top at the source point (see Fig. 2). The pyramid is limited by the scattering planes in the two-beam cases.

If $L \neq 0$, then two-beam stripes arise on the topograph which correspond to the two-beam stripes on the $\mathbf{q}$ plane, in accordance with (18). These stripes are perpendicular to the corresponding reciprocal-lattice vectors if the film plane is parallel to the plane of reciprocal-lattice vectors. It follows from the calculations that a maximum of intensity inside the hexagon lies near the top of a hexagon corresponding to a forward direct beam. The sum of two patterns, corresponding to multiple diffraction and two-beam diffraction for the strong reflections 220 and $\bar{2}02$, gives rise to the peculiarity on the topographs (semicircular arcs at one side of the intersection of 220 and $\bar{2}02$ stripes) found by Umeno (1970, 1972).

2.4. *Focusing*

From (26), for each stationary-phase point q_{ij} it is possible to focus X-rays if $C_m > 0$ and $t = C_m^{-1} L$. For finding the stationary-phase points q_{ij} and coefficients C_m the derivatives $(\partial\delta/\partial q_k)$ and $(\partial^2\delta/\partial q_k\,\partial q_l)$ have to be known. In the general case, the solution of the eigenvalue problem (5) is obtained only by means of numerical methods. Hence, the following expression for the derivatives, corresponding to the first and second orders of the perturbation series in a small parameter dq, becomes very useful (Kohn, 1976):

$$\partial\delta^{(j)}/\partial q_k = \sum_{\substack{nm \\ ss'}} B_{ns}^{(j)}(q)[\partial G/\partial q_k]_{nm}^{ss'} B_{ms'}^{(j)}(q)$$

$$\equiv \langle j|\partial G/\partial q_k|j\rangle, \tag{29}$$

$$\partial^2\delta^{(j)}/\partial q_k\,\partial q_l = 2\sum_{j\neq j'} \langle j'|\partial G/\partial q_k|j\rangle\langle j'|\partial G/\partial q_l|j\rangle \times (\delta^{(j)} - \delta^{(j')})^{-1} \tag{30}$$

Taking into account the explicit form of the matrix G [see Pinsker (1978), p. 442] and (29) and (30), one may easily obtain $(\partial\delta/\partial q) \simeq K^{-1}$ and $(\partial^2\delta/\partial q^2) \simeq K^{-2}\Delta^{-1}$, where $\Delta = \min(\delta^{(j)} - \delta^{(j')})$. The magnitude of the parameter Δ can be evaluated as $g|\chi_h|$, where χ_h is the Fourier transform of the crystal polarizability for the reciprocal-lattice vector $\mathbf{h}$ with a maximum magnitude ($|\chi_h| \simeq 10^{-5}$) and g is a numerical factor ($g < 1$). Then from (13), (16) and (27) we obtain $C_m > |\chi_h|^{-1} \simeq 10^5$. The denominator of (24) can be changed for L only if $L \gg Ct$, where $C = \max(C_1, C_2)$. For example, the distance L should exceed 50 m for a crystal of 0·2 mm thickness. This distance is very difficult to achieve in the experiment. We note that the evaluation obtained is correct only for the multiple-diffraction angular region. In the one-beam region the coefficients C_m fall to zero. In the two-beam angular regions more detailed analysis has been carried out by Afanas'ev & Kohn (1977*a*) and Aristov *et al.* (1980).

The physical reason for the existence of two focusing distances for any angular region (in contrast with the two-beam case, where only one focusing distance exists) arises from the more complicated form of the dispersion surface. In the two-beam case the dispersion surface is cylindrical. If two or more cylinders intersect, there is a region with nonzero curvature in two directions. The curvature radii are different for different directions in the general case. The existence of two different radii of curvature is sufficient to give rise to the two focusing distances. Focusing takes place if the DS curvature is compensated by the curvature of the constant-phase surface of the Fourier transform of the spherical wave.

3. Computational aspects

Although the computation of the intensity by means of (13), (18), (20) and (24)–(27) is simpler than a computation using the rigorous expressions (6)–(8), it requires a certain amount of effort. The roots of (18), *i.e.* the points q_{ij}, are difficult to determine numerically at every point x because they have different values for the different zones of the DS. On the other hand, the methods of matrix diagonalization give all the zones of the DS at once. In order to solve the problem by computer, we use the following algorithm.

In the first stage, the eigensolution problem (5) is solved and the values of $I_{0j}^{pw}(q, t)$, $(\partial\delta^{(j)}/\partial q_k)$ and $(\partial^2\delta^{(j)}/\partial q_k\partial q_l)$ are calculated for some fixed value of t and some set of q_n which are chosen, for example, as nodes of the rectangular lattice in the q plane. In the second stage, the points x_n are calculated which correspond directly to q_n *via* (18) for some fixed value of L. The points x_n are the nodes of a curvilinear

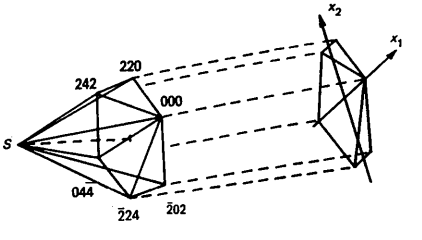

Fig. 2. Six-beam pyramid and its projection on the film plane.

lattice in a general case. Moreover, the correspondence $q \triangleq x$ may not be single valued, so that different regions in the q plane may give the same region in the x plane.

In the third stage, the values of (24) are calculated by linear interpolation of the quantities $I_{0j}^{pw}(q, t)$ and $(\partial^2\delta^{(j)}/\partial q_k \partial q_l)$ at the nodes of some fixed rectangular lattice in the x plane. The values of the third derivative of $\delta^{(j)}$ are calculated approximately. The interpolation is carried out in the following way. All the triangles of the lattice in the q plane are examined for a fixed point in the x plane. The triangle in the x plane is found which corresponds to each triangle in the q plane and has arbitrary shape in the general case. If the given x point lies inside the triangle, the interpolation is made, otherwise the next triangle is considered. If after the examination of all the triangles this condition is not fulfilled, zero intensity is attributed to this point. If the condition is fulfilled repeatedly, the results are added. The results from different zones of the DS are added similarly.

The algorithm described above is still not convenient because it is necessary to remember the results of the computation for a very great number of points in the first stage. Actually, one can avoid this difficulty by taking fixed values of L and t as well as the rectangular lattice in the x plane in the first stage and then considering the q plane step by step.

4. Numerical results

The computation has been carried out for the case of six-beam (220/242/044/$\bar{2}$24/$\bar{2}$02) diffraction of Cu $K\alpha$ radiation ($\lambda = 0{\cdot}154$ nm) in a Ge crystal. This case was first analysed theoretically by Joko & Fukuhara (1967). They pointed out that a strong reduction of the absorption coefficient takes place in the case of exact multiple diffraction, where all the Bragg conditions are satisfied strictly. This has been shown more correctly by Afanas'ev & Kohn (1977*b*).

Huang, Tillinger & Post (1973) have investigated this case both experimentally and theoretically. In the experiment the effect of enhancement of the anomalous transmission has not been found. As for theoretical calculations, the plane-incident-wave angular dependence of the transmission coefficient (ADTC) is incorrect. Indeed, the ADTC calculated by Huang *et al.* (1973) is symmetrical both in the direction lying in the scattering plane for the 044 reflexion (the $\mathbf{e}_{0\pi}$ direction) and in the normal direction (the $\mathbf{e}_{0\sigma}$ direction). But, as is well known, the ADTC is asymmetrical in an absorbing crystal even in the two-beam case (see *e.g.*, Pinsker, 1978, p. 110).

The correct pattern of ADTC was first obtained by Kohn (1976) and then by Mihailyuk, Kshevetskii, Ostapovich & Kozmik (1978). Kohn (1976) has pointed out that the ADTC calculated by Huang *et al.* (1973) is incorrect because the ADTC has been found to be strongly asymmetrical in the $\mathbf{e}_{0\pi}$ direction. This asymmetry, in particular, is revealed in the asymmetrical intensity distribution on the topographs in the case where $L = 0$, which is the reason for the effect observed by Umeno (1970, 1972). However, a recent publication by Chang (1982) again contains the incorrect results for the ADTC in this case.

In the present work the angular dependence of quantities which enter the computational formulae is accounted for in the region shown in Fig. 3. The two-beam stripes are long enough for computing the topographs for all the L values considered. The dimensions of the central rectangle are determined by the inequalities $|\theta_1| \leq 0{\cdot}23$, $|\theta_2| \leq 0{\cdot}05$ mrad. The angle θ_1 changes along the vector $\mathbf{e}_{0\pi}$ (horizontal line) and θ_2 changes along $\mathbf{e}_{0\sigma}$ (vertical line). The distances between the points in the angular plane are different. The smallest distance is $\simeq 0{\cdot}001$ mrad in the central part. In the two-beam stripes the points form a lattice with a parallelepiped as a unit cell and with a variable step. The total number of points in which the

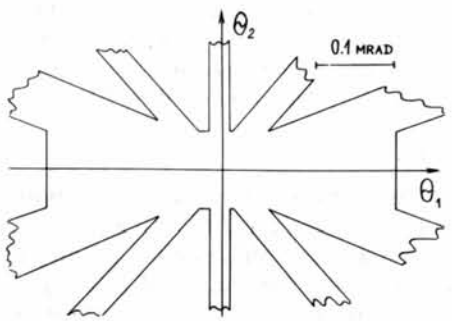

Fig. 3. The central part of the angular region taken into account in computations.

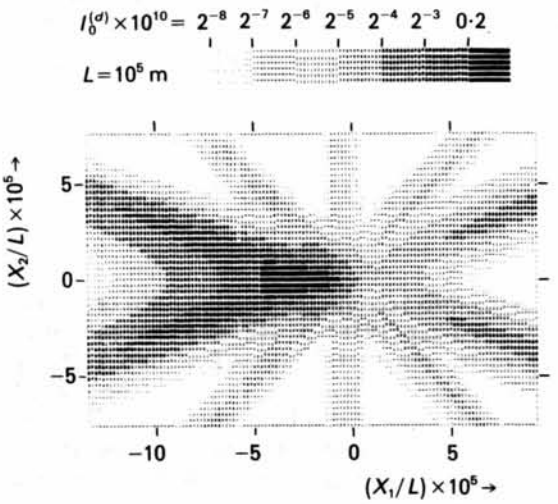

Fig. 4. The forward direct-beam topograph computed in the case of six-beam (220/242/044/$\bar{2}$24/$\bar{2}$02) diffraction of Cu $K\alpha$ radiation in a Ge crystal of thickness 0·2 mm. The distance between the source and the film $L = 10^5$ m.

eigensolution problem (5) was solved is approximately 2500. The data for calculations were taken from the paper by Kohn (1976).

Figs. 4–8 show the computed topographs for $t=0{\cdot}2$ mm and $L=10^5$ m (Fig. 4), 6 m (Fig. 5), 2 m (Fig. 6), 1 m (Fig. 7) and 0·5 m (Fig. 8). The origin in Figs. 5–8 is chosen at the centre of the hexagon on the topograph for $L=0$ (see Fig. 2). Fig. 4 corresponds to the anomalously large distance between source and film. It actually shows the ADTC in the central angular region. The asymmetry in the horizontal direction of the multiple-diffraction angular region and the two-beam stripes is seen quite well. It should be mentioned that the maximum of intensity turns out to be at the left side of the intersection of the two-beam stripes. This result was formerly obtained by Kohn (1976) and Mihailyuk *et al.* (1978). The width of the two-beam stripes is proportional to $|\chi_{rh}|/\sin 2\theta_B$, where χ_{rh} is the Fourier transform of the real part of the crystal polarizability and θ_B is the Bragg angle for two-beam diffraction. Consequently, the 220 stripe is noticeably wider than the 224 stripe, and the 224 stripe in turn is wider than the 044 stripe.

The theoretical topograph for a relatively large distance $L=6$ m is shown in Fig. 5. It is easy to see that the structure of the multiple-diffraction region changes sharply. The two-beam stripes are shown only in the central part of the topograph where they are distorted to a considerable extent by the multiple-diffraction effect. In particular, the 220 and 224 stripes have not arisen on the right of the topograph. However, it is easily seen at the left part of the topograph that the 224 stripe has a narrow core of great intensity. This is due to the focusing effect predicted by Afanas'ev & Kohn (1977*a*) and seen experimentally by Aristov *et al.* (1978), Kozmik & Mihailyuk (1978) and Aristov *et al.* (1980) in the simpler two-beam case.

Table 1. *Focusing distances for the two-beam stripes in a six-beam geometry for a crystal of* 0·2 *mm thickness*

hkl	220	220	224	044	044	224
s	σ	π	σ	σ	π	π
$L_{foc}(m)$	3·67	5·22	10·14	11·47	61·32	92·62

In this case the coefficients $C_m^{(j)}$ of (27) are positive only for the slightly absorbing zones of the DS. According to Afanas'ev & Kohn (1977*a*), they are determined by

$$C^{(j)}=(\sin^2 2\theta_B)/2\gamma_0|\chi_{rh}||P_j| \qquad (31)$$

if the Bragg condition is satisfied exactly. Here j stands for a polarization index (σ or π) and P_j is a polarization factor which has the value 1 for σ polarization and $\cos 2\theta_B$ for π polarization. The values of distance $L_{\rm foc}$, corresponding to focusing the divergent radiation by a crystal plate of $t=0{\cdot}2$ mm, can easily be calculated with (31) and are shown in Table 1.

Anomalously small dimensions of the central spot are another effect of focusing the considerable number of zones of the multiple-diffraction DS. Indeed, if $L=0$, the radiation is concentrated in a crystal inside the six-beam pyramid (see Fig. 2). This leads to topograph dimensions of approximately 0·3 × 0·4 mm. In the case of $L=6$ m we supposed that the dimensions of the multiple-diffraction region would increase but it follows from a computation that the dimensions of the central spot are 0·15 × 0·15 mm. A large region of low intensity on the right of the topograph also arises from this cause.

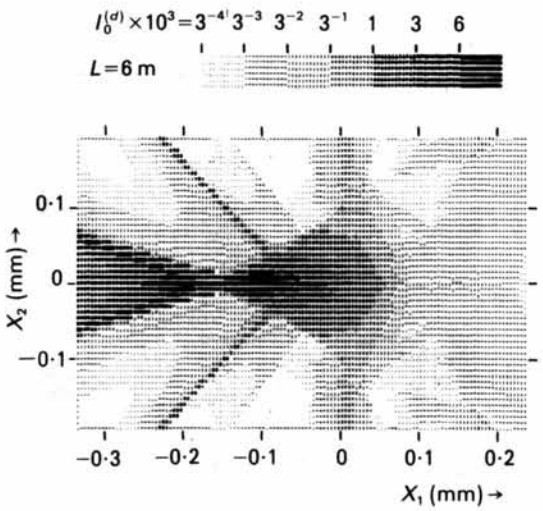

Fig. 5. Computed topograph for the same conditions as in Fig. 4, but with $L=6$ m.

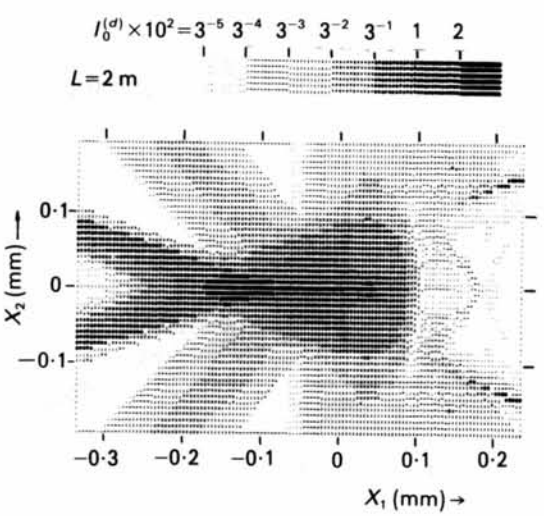

Fig. 6. Computed topograph for the same conditions as in Fig. 4, but with $L=2$ m.

From the above discussion, it is not difficult to understand the peculiarities of the topograph shown in Fig. 6. We note that in papers by Kshevetskii & Mihailyuk (1976) and Mihailyuk *et al.* (1978) the experimental (positive) topographs were obtained for the same parameters. In the experiment nonmonochromatic radiation was used. The wavelength band was of the order of the natural width of the Cu $K\alpha$ spectral line. As a result, the patterns were averaged within a region ~0·5 mm in a horizontal direction according to Kohn (1976). Nevertheless, the region with low intensity on the right of the topographs was obtained, but the central multiple-diffraction region was seen as a narrow horizontal bright stripe. The authors connected this result with the anomalous transmission enhancement effect. However, it follows from our calculation that they have seen the effect of three-beam (220/$\bar{2}$02) focusing on the background of the particularly strongly focusing two-beam 220 and $\bar{2}$02 stripes. The 242 and 044 stripes in Fig. 6 are wider than the 220 stripe.

The topograph in Fig. 7 corresponds to $L = 1$ m. As follows from the computations, in this case all the two-beam stripes become fainter and wider (defocusing). The central intensity distribution corresponding to the multiple diffraction acquires little by little the form of a projection of the base of a six-beam pyramid (see Fig. 2) as L is decreased. The intensity maximum on the left of the topograph arises, as before, from focusing the two-beam lines of ADTC, but in a longitudinal direction. In other words, they are attracted to the centre of the topograph. As for the small angular region corresponding to the pure multiple-diffraction effect, we note that the corresponding plane waves are strongly scattered inside the six-beam pyramid. This is why the strong reduction of the absorption coefficients does not show up on the topographs.

Indeed, the zones of the DS corresponding to the anomalous transmission have a very great curvature. As has been shown by Kohn (1976), there are few zones of this kind and the distances between them $[\delta^{(j)} - \delta^{(j')}]$ are very small. Then, according to (30), the denominator of (24) has a large value which leads to a decrease in the intensity. The other consequence of the DS curvature is the relatively small value of the derivative (dq_{ij}/dx) in (24). Therefore, the energy flow in a narrow cone with angular sizes of order 0·005 mrad near κ_0, corresponding to these zones, is highly scattered in the crystal, filling almost the whole six-beam pyramid (Fig. 2).

In the topograph of Fig. 8 ($L = 0{\cdot}5$ m) the peculiarities pointed out above are still clearer. For smaller values of L the intensity maximum corresponding to the multiple diffraction passes to the right of the intersection of the two-beam lines. These lines become still more intense and hide the multiple-diffraction region. This is because of the absence of angular dependence of the intensity along the two-beam lines. As a result, the intensity of two-beam lines increases as L^{-1} with a decrease in L, but the intensity of multiple-diffracted X-rays does not depend on L. Then the six-beam diffraction effect is revealed on the topographs very peculiarly by arcs to the right of the 220 and $\bar{2}$02 two-beam lines. Just the same pattern has been obtained by Umeno (1970, 1972). Despite the fact that this peculiarity can be seen even in Fig. 8, the smaller value of L is necessary for experimental studies. Only for small values of L does the averaging of the topograph owing to the nonmonochromaticity of radiation become small. This case will be considered in more detail in a separate paper.

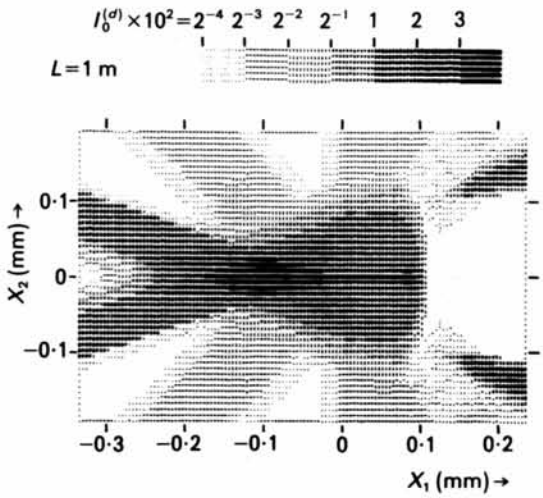

Fig. 7. Computed topograph for the same conditions as in Fig. 4, but with $L = 1$ m.

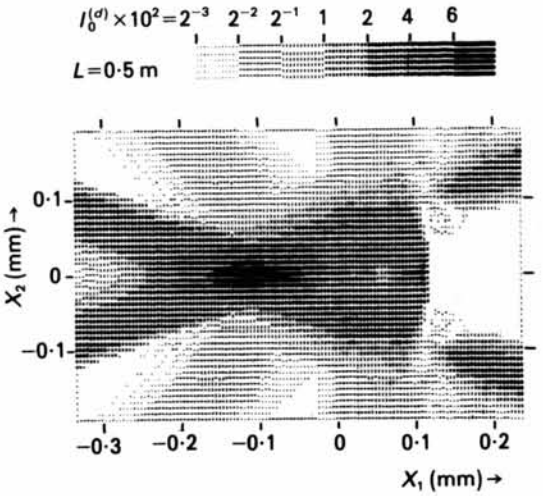

Fig. 8. Computed topograph for the same conditions as in Fig. 4, but with $L = 0{\cdot}5$ m.

5. Concluding remarks

The investigation we have carried out demonstrates that the multiple diffraction of X-ray spherical waves (six-beam in particular) is a very complicated phenomenon. More systematic studies, both theoretical and experimental, are necessary. The intensity distribution on the topograph depends to a great extent on the distance between the source and the film. Since nonmonochromatic radiation has been used in the experiments it is impossible to compare the topographs in the forward-transmitted beam with the experimental topographs. Nevertheless, there is qualitative agreement. In order to reveal the fine structure of the experimental topographs it is desirable to use monochromatic radiation.

References

AFANAS'EV, A. M. & KOHN, V. G. (1977*a*). *Fiz. Tverd. Tela*, **19**, 1775–1783.

AFANAS'EV, A. M. & KOHN, V. G. (1977*b*). *Acta Cryst.* A**33**, 178–184.

ARISTOV, V. V., POLOVINKINA, V. I., AFANAS'EV, A. M. & KOHN, V. G. (1980). *Acta Cryst.* A**36**, 1002–1013.

ARISTOV, V. V., POLOVINKINA, V. I., SHMYT'KO, I. M. & SHULAKOV, E. V. (1978). *Pis'ma Zh. Eksp. Teor. Fiz.* **28**, 6–9.

BALTER, S., FILDMAN, R. & POST, B. (1971). *Phys. Rev. Lett.* **27**, 307–310.

CHANG, S.-L. (1982). *Z. Naturforsch. Teil A*, **37**, 501–504.

HUANG, T. C. & POST, B. (1973). *Acta Cryst.* A**29**, 35–37.

HUANG, T. C., TILLINGER, H. H. & POST, B. (1973). *Z. Naturforsch. Teil A*, **28**, 600–603.

JEFFREYS, H. & SWIRLES, B. (1966). *Methods of Mathematical Physics.* Cambridge Univ. Press.

JOKO, T. & FUKUHARA, A. (1967). *J. Phys. Soc. Jpn*, **22**, 597–604.

KATO, N. (1961). *Acta Cryst.* **14**, 627–636.

KATO, N. (1968). *J. Appl. Phys.* **39**, 2225–2230.

KOHN, V. G. (1976). *Fiz. Tverd. Tela*, **18**, 2538–2545.

KOHN, V. G. (1977). *Fiz. Tverd. Tela*, **19**, 3567–3574.

KOZMIK, V. D. & MIHAILYUK, I. P. (1978). *Ukr. Fiz. Zh.* **23**, 1570–1571.

KSHEVETSKII, S. A. & MIHAILYUK, I. P. (1976). *Kristallografiya*, **21**, 381–382.

MIHAILYUK, I. P., KOZMIK, V. D. & KSHEVETSKII, S. A. (1977). *Ukr. Fiz. Zh.* **22**, 224–229.

MIHAILYUK, I. P., KSHEVETSKII, S. A., OSTAPOVICH, M. V. & KOZMIK, V. D. (1978). *Kristallografiya*, **23**, 403–405.

PINSKER, Z. G. (1978). *Dynamical Scattering of X-rays in Crystals.* Heidelberg, London, New York: Springer-Verlag.

UMENO, M. (1970). *Phys. Status Solidi A*, **2**, K203–K205.

UMENO, M. (1972). *Phys. Status Solidi A*, **11**, 501–511.

Acta Cryst. (1986). A**42**, 449–456

Modified Two-Beam Description of X-ray Fields and Intensities near a Three-Beam Diffraction Point. Second-Order Solution

BY HELLMUT J. JURETSCHKE

Polytechnic Institute of New York, 333 *Jay Street, Brooklyn, New York* 11201, *USA*

(*Received* 18 *February* 1986; *accepted* 2 *April* 1986)

Abstract

The previously developed first-order modification of two-beam diffraction near a third reciprocal-lattice point [Juretschke (1984). *Acta Cryst.* A**40**, 379–389] is extended to second order. To this order a modified two-beam description is still retainable, and the normal modes persist in their original polarization, but now with respect to two-beam asymptotes rotated and with a Bragg angle altered relative to the original two-beam case. Integrated intensities are evaluated for modified strong and weak primary two-beam symmetric Bragg reflections, in the Bragg–Bragg and Bragg–Laue configurations, and some implications of the results are discussed.

1. Introduction

A compact analytical description of X-ray modes and intensities in the neighborhood of multiple-interaction regions would have practical as well as theoretical uses. Among other things, it would allow the evaluation of the influence of additional nearby reflections on a particular reflection of interest without having to invoke the computer machinery of a full n-beam solution. Equally well, it would lead to easy identification of particular features of diffraction, such as the traditional *Aufhellung*, or *Umweganregung*, using relatively simple rules.

The first-order formulation of such a description (Juretschke, 1982, 1984; Høier & Marthinsen, 1983), based on a systematic perturbation treatment of the n-beam equations, has already been applied successfully to clarify some old problems (Juretschke & Barnea, 1986; Juretschke & Wagenfeld, 1986), as well as to predict additional results (Juretschke, 1986*a*, *b*). In the course of these investigations, however, a number of instances emerged in which this first-order formulation led to null results, or where it applied in only a very limited domain, so that the dominant

0108-7673/86/060449-08$01.50